Two-dimensional Peierls-Hubbard model within the slave-boson approach

H. Fehske, M. Deeg, and H. Büttner
Physikalisches Institut, Universität Bayreuth, D-8580 Bayreuth, Germany
(Received 22 August 1991; revised manuscript received 10 February 1992)

We have used a slave-boson formulation of the Peierls-Hubbard model on a square lattice to study the stability of the ground state against a static (π,π) lattice displacement. At half-filling our saddle-point solutions give a stable paramagnetic state with an on-site frozen-in breathing mode accompanied by a commensurate charge-density wave above a critical electron-phonon coupling strength. The transition to the "dimerized" state is suggested to be of first order. Increasing the Coulomb interaction, one observes a monotonous decrease of the static displacement amplitude. In order to map out the phase diagram of the Peierls-Hubbard model away from half filling, we first discuss the relative stability of several homogeneous phases, including para-, ferro-, ferri-, and antiferromagnetic states with and without lattice distortion. Parameter regions exist where magnetic order is stabilized by the local electron-phonon coupling. Allowing the existence of heterogeneous solutions, i.e., mixed phases, we show that phase-separated states are lowest in energy over a wide range of hole density and interaction strength.

I. INTRODUCTION

Superconductivity in the high-T_c layered copper oxides[1] raises again the question concerning the effect of electron-phonon interaction in strongly correlated fermion systems. The role of electron-phonon coupling is of special interest in view of the close proximity of these materials, i.e., $La_{2-x}Ba_xCuO_4$, to structural, insulating antiferromagnetic, and superconducting instabilities. Starting from an effective Hubbard model,[2] the antiferromagnetism of the undoped parent compounds can be understood as electronic correlation effects in a half-filled band. Upon doping, a transition to a metallic phase takes place, where the motion of the charge carriers is strongly affected due to the coupling on the fluctuating (copper) spin background.[3] Simultaneously, close to half filling, the two-dimensional (2D) tight-binding band structure gives rise to Fermi-surface nesting, leading to a charge-density-wave (CDW) instability. Thus a local electron-phonon interaction may be of special importance and one can speculate whether the renormalized quasiparticle band is also unstable against a CDW formation driven by a frozen-in oxygen breathing mode.[4,5] Along this line, polaronic or bipolaronic theories of superconductivity have been developed.[5-8] Besides the possible relevance of the Peierls-Hubbard model to the physics of high-T_c superconductors, it is an important issue to study the interdependence of electron-electron and electron-lattice interaction on a 2D system in the normal phase. The stability of the 2D Hubbard model against static lattice displacements (or "dimerization") was investigated for the local Holstein coupling[9] using a simple Hartree-Fock approximation[5] as well as quantum Monte Carlo (QMC) technique,[10] and for an electron-phonon coupling to the electronic hopping term with exact diagonalization and perturbation methods.[11,12]

II. THEORETICAL FORMULATION

In this paper, we present a slave-boson (SB) mean-field study of the ground-state properties ($T=0$) of the 2D Peierls-Hubbard model, taking into account various symmetry broken states compatible with the underlying bipartite lattice.

Our approach is based on the following effective one-band Hamiltonian:

$$H=\sum_{i,j,\sigma} t_{ij}c_{i\sigma}^{\dagger}c_{j\sigma}+U\sum_i c_{i\uparrow}^{\dagger}c_{i\uparrow}c_{i\downarrow}^{\dagger}c_{i\downarrow} -\alpha\sum_{i,\sigma} q_i c_{i\sigma}^{\dagger}c_{i\sigma}+\frac{k}{2}\sum_i (x_i^2+y_i^2)\ , \tag{1}$$

where $c_{i\sigma}^{\dagger}$ ($c_{i\sigma}$) are the usual fermonic creation (destruction) operators at Wannier site i with spin σ. t and U denote the transfer amplitude restricted to nearest-neighbor hopping processes on a square lattice and the on-site part of the Coulomb repulsion, respectively. The electronic system is coupled to the Holstein coordinates q_i via a local electron-phonon coupling α, where the phonon modes are treated in the adiabatic approximation. The Hamiltonian (1) was proposed by Prelovšek, Rice, and Zhang[5] to be appropriate to the theoretical description of particular breathing modes in the CuO_2 planes of La_2CuO_4. In this case, one has $q_i=(x_{i_x,i_y}-x_{i_x-1,i_y}+y_{i_x,i_y}-y_{i_x,i_y-1})/4$ where x_i,y_i correspond to the displacements of both O atoms in the unit cell $i=(i_x,i_y)$ in a harmonic lattice with spring constant k. In the following, all energies are measured in units of t and we introduce a dimensionless electron-phonon coupling constant $\lambda=\alpha^2/16k$, as in Ref. 5. Treating the Hubbard interaction in the Hartree-Fock approximation, one gets in the limit $\lambda<1$ from a continuous version of (1) a stable CDW state for $U<U_0=8\lambda$.[5,13] The QMC simu-

lations show a departure from the simple mean-field results at larger U and finite doping.[10]

To handle the cases of weak, intermediate, and strong electron-electron as well as electron-phonon coupling on the same footing, we use in our nonperturbative treatment the SB method in the version of Kotliar and Ruckenstein.[14] Their auxiliary boson approach allows a unique treatment of para- (PM), ferro- (FM), ferri- (FIM), and antiferromagnetic (AFM) long-range order, spiral magnetic states,[15] and metal-insulator transitions. The SB technique leads to a quantitative agreement with QMC calculations over a wide range of interactions and doping.[16] The theory is readily generalized to a spin rotation invariant form[17] and to the incorporation of electron-phonon coupling.[18]

In analogy to Ref. 14 we enlarge the physical Hilbert space of fermion states at each site, introducing four auxiliary boson operators, where $e_i^\dagger$ (e_i), $p_{i\sigma}^\dagger$ ($p_{i\sigma}$), $d_i^\dagger$ (d_i) creates (destroys an empty, a single occupied (spin σ), and a double occupied state at site i. The unphysical states in the extended Fock space are eliminated by imposing a set of local constraints,

$$e_i^\dagger e_i + p_{i\uparrow}^\dagger p_{i\uparrow} + p_{i\downarrow}^\dagger p_{i\downarrow} + d_i^\dagger d_i = 1 \quad \text{(completeness)}$$

and

$$p_{i\sigma}^\dagger p_{i\sigma} + d_i^\dagger d_i = c_{i\sigma}^\dagger c_{i\sigma}$$

(fermion occupancy of a given spin).

Then the grand-canonical partition function can be expressed by a multiple path integral over fermion (anticommuting) and boson (commuting) fields as

$$Z = \int D[e^*,e]D[p_\sigma^*,p_\sigma]D[d^*,d]D[c_\sigma^*,c_\sigma] \times D[q]D[\lambda^{(1)}]D[\lambda_\sigma^{(2)}]e^{-S} \tag{2}$$

with the action

$$S = \int_0^\beta d\tau \sum_i \left\{ e_i^* \partial_\tau e_i + d_i^* \partial_\tau d_i + \sum_\sigma \left[p_{i\sigma}^* \partial_\tau p_{i\sigma} + c_{i\sigma}^* (\partial_\tau - \mu) c_{i\sigma} \right] + \lambda_i^{(1)} \left[e_i^* e_i + d_i^* d_i + \sum_\sigma p_{i\sigma}^* p_{i\sigma} - 1 \right] + \sum_\sigma \lambda_{i\sigma}^{(2)} (c_{i\sigma}^* c_{i\sigma} - p_{i\sigma}^* p_{i\sigma} - d_i^* d_i) + U d_i^* d_i + \frac{k}{2}(x_i^2 + y_i^2) + \sum_{j,\sigma} c_{i\sigma}^* (t_{ij} z_{i\sigma}^* z_{j\sigma} - \alpha q_i \delta_{ij}) c_{j\sigma} \right\} . \tag{3}$$

where the time-dependent Lagrange multipliers $\lambda_i^{(1)}, \lambda_{i\sigma}^{(2)}$ are introduced to enforce the constraints. The projectors

$$z_{i\sigma} = (1 - d_i^* d_i - p_{i\sigma}^* p_{i\sigma})^{-1/2} (e_i^* p_{i\sigma} + p_{i-\sigma}^* d_i)(1 - e_i^* e_i - p_{i-\sigma}^* p_{i-\sigma})^{-1/2}$$

ensure the correct saddle-point behavior of (2) in the limit of the vanishing Coulomb interaction.[14]

Due to the bipartite structure of the square lattice, let us separate the crystal into two sublattices indicated by $\eta = A, B$. The free Fermi-surface nesting vector (π,π), the AFM order vector (π,π), and the possibility of a frozen-in (breathing) phonon mode with the same wave vector related to a CDW-Peierls instability suggest the appearance of such symmetry broken ground states at least at half filling. Evaluating the partition function (2), one perform the Gaussian integral over the Grassmann fields.[19] At the two sublattice mean-field level, the boson fields are considered as static and uniform on each sublattice η. This approximation reduces the bosonic functional integral to the evaluation of the integrand at the saddle point. At the same time, the constraints can be satisfied on each sublattice only on average. The grand-canonical potential per site then follows as

$$\tilde{f} = \tfrac{1}{2} \sum_\eta \left\{ \lambda_\eta^{(1)} e_\eta^2 + \sum_\sigma (\lambda_\eta^{(1)} - \lambda_{\eta\sigma}^{(2)}) p_{\eta\sigma}^2 + (\lambda_\eta^{(1)} - \lambda_{\eta\uparrow}^{(2)} - \lambda_{\eta\downarrow}^{(2)} + U) d_\eta^2 - \lambda_\eta^{(1)} + \Delta^2/16\lambda \right\} - \frac{1}{\beta N} \sum_{\mathbf{k},\nu,\sigma} \ln \left\{ 1 + e^{-\beta(\varepsilon_{\mathbf{k},\nu,\sigma} - \mu + \lambda_\sigma^{(2)})} \right\} , \tag{4}$$

where the renormalized single-particle energies ($\nu = \pm 1$)

$$\varepsilon_{\mathbf{k}\nu\sigma} = \nu \left[\left[\frac{\lambda_{A\sigma}^{(2)} - \lambda_{B\sigma}^{(2)}}{2} - \Delta \right]^2 + \varepsilon_{\mathbf{k}}^2 |z_{A\sigma}|^2 |z_{B\sigma}|^2 \right]^{1/2} \tag{5}$$

are obtained by the Fourier transformation of the kinetic part. Here $\beta = 1/k_B T$, $\lambda_\sigma^{(2)} = (\lambda_{A\sigma}^{(2)} + \lambda_{B\sigma}^{(2)})/2$, and the $\mathbf{k}$ summation is restricted to the magnetic Brillouin zone of the square lattice. Further, we have used the convenient notation $\alpha q_i = \xi_\eta \Delta$, where $\xi_\eta = +1$ (-1) if site i belongs to the A, (B) sublattice, introducing the gap parameter[5] Δ. Note that the elastic energy can now be expressed as a quadratic form in the Holstein coordinate.

Requiring the thermodynamic potential to be stationary with respect to variations of the mean-field parameters e_η, d_η, $p_{\eta\sigma}$, $\lambda_\eta^{(1)}$, $\lambda_{\eta\sigma}^{(2)}$, and Δ, one has to solve a set of 15 coupled self-consistency equations to get the saddle-point values of the bosonic fields. In particular, the ex-

tremal equation of the static displacement (or gap parameter) Δ are obtained as

$$\Delta=8\lambda\frac{1}{N}\sum_{\mathbf{k},\nu,\sigma} n_{\mathbf{k}\nu\sigma}\frac{1}{\varepsilon_{\mathbf{k}\nu\sigma}}\left\{\frac{\lambda^{(2)}_{A\sigma}-\lambda^{(2)}_{B\sigma}}{2}-\Delta\right\} \tag{6}$$

with

$$n_{\mathbf{k}\nu\sigma}=\frac{1}{e^{\beta(\varepsilon_{\mathbf{k}\nu\sigma}-\mu+\lambda^{(2)}_{\sigma})}+1}\ . \tag{7}$$

Let us emphasize that Δ is (via $\varepsilon_{\mathbf{k}\nu\sigma}$) contained implicitly in all other optimization equations. We determine the saddle-point fields numerically at $T=0$, using the 2D tight-binding density of states. At given electron (hole) density n (δ), the chemical potential μ is fixed by the requirement

$$n=1-\delta=\frac{1}{N}\sum_{\mathbf{k},\nu,\sigma} n_{\mathbf{k}\nu\sigma}\ , \tag{8}$$

where the sublattice particle numbers are given by $n_\eta=n+\xi_\eta\Delta/8\lambda$. By employing the formalism so far, we searched in the numerical work for PM, AFM, FM, and FIM solutions with and without Δ. The physically relevant saddle point is determined to give the lowest free energy per site

$$f=\tilde{f}+\mu n\ . \tag{9}$$

However, our procedure allows the investigation of metastable solutions corresponding to local minima in the 15-dimensional variational space of the free energy.

III. NUMERICAL RESULTS AND DISCUSSION

A. The $\delta=0$ case

Starting at half-filling ($\delta=0$), the static lattice displacement Δ and the free energy of various phases are plotted in Fig. 1 as a function of U at different λ. Obviously, the solution with finite Δ leads to the lowest free energy below a critical ratio U/λ; i.e., including a local electron-phonon interaction, the AFM saddle point[14–16] is unstable against a PM "dimerized" state. In agreement with exact diagonalization results[12] for finite 2D lattices with a Su-Schrieffer-Heeger coupling,[20] the gap parameter Δ is a monotonous decreasing function of the Coulomb interaction. The abrupt breakdown of Δ at U_c indicates a first-order phase transition, where at small λ the critical value U_c agrees well with the Hartree-Fock value U_0. If the electron-phonon coupling strength is raised, U_c deviates from U_0 ($U_c<U_0$; cf. the QMC results of Ref. 10), and one observes a metastable "dimerized" solution at $U>U_c$. The portions of empty, single, and double occupied sites are shown for the A sublattice in Fig. 2. In the AFM phase, the staggered magnetization follows from $m_\eta=p^2_{\eta\uparrow}-p^2_{\eta\downarrow}$. Here we are able to test our numerical procedure at $U=4$ by reproducing the sublattice magnetization results of Frésard, Dzierzawa, and Wölfle.[15] In the "dimerized" state the site energies of the A (B) lattice are lowered (raised), which leads to an increase (decrease) of double occupied sites, i.e., a

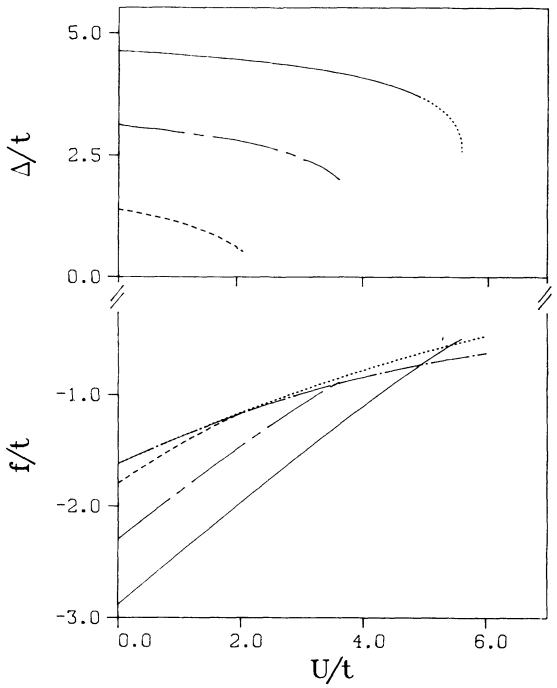

FIG. 1. Static lattice displacement Δ (upper half) and free energy per site f (lower half) as a function of the Coulomb repulsion U for the half-filled band case ($\delta=0$). The results are given at various electron-phonon coupling strengths $\lambda=0.625$ (full line), $\lambda=0.45$ (chain dashed line), and $\lambda=0.25$ (dashed line). The free energies are compared with systems without electron-phonon coupling, namely the PM state (dotted) and the AFM state (chain dotted). The dotted region in Δ vs U corresponds to a metastable solution of the saddle-point equations.

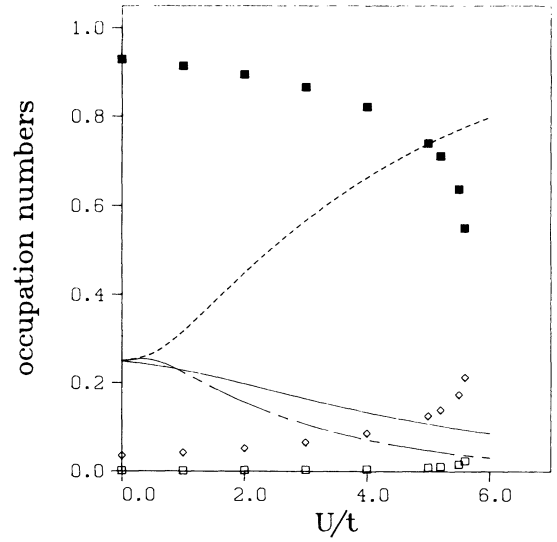

FIG. 2. Probability (occupation number) in the "dimerized" state for an empty (□), a double occupied (■), and a single occupied site with spin projection up (◇) or down (△), on the A sublattice at half filling for $\lambda=0.625$. The corresponding probabilities e^2_A (dotted curve), d^2_A (full curve), $p^2_{A\uparrow}$ (dashed curve), and $p^2_{A\downarrow}$ (chain dashed curve) are shown for the "undimerized" AFM phase where $e^2_A=d^2_A$ at $\delta=0$.

Peierls CDW. Increasing U, the energy cost at double occupied sites starts to dominate the energy gain on the A lattice through "dimerization" until the AFM is established at U_c, restoring the symmetry $n_A = n_B$.

The variation of Δ with λ at fixed $U=4$ shown in Fig. 3 again illustrates the first-order transition behavior. The region below λ_c, where we found metastable "dimerized" solutions, increases with U. In the case of vanishing electron-electron interaction one has an instability to a lattice-distorted state even at infinitesimal λ. Obviously $\Delta(\lambda)$ tends to the asymptote $\Delta = 8\lambda$ in the opposite limit of very large electron-phonon coupling, where all electrons rest on the same sublattice.

In order to discuss the mobility of the charge carriers we have calculated in Fig. 4 the effective hopping matrix element

$$t_{\text{eff}} = \frac{\left\langle \sum_{i,j} c_{i\sigma}^{\dagger} c_{j\sigma} \right\rangle}{\left\langle \sum_{i,j} c_{i\sigma}^{\dagger} c_{j\sigma} \right\rangle_{U=0,\lambda=0}} . \tag{10}$$

This quantity was investigated by Lilly, Muramatsu, and Hanke[16] within SB mean-field theory for the pure Hubbard model, to demonstrate the interpolating character of this theory over a wide range of interaction strength as well as the excellent quantitative agreement with QMC results. Due to the large number of double occupied sites on the A sublattice, the effective hopping amplitude is reduced in the "dimerized" state compared to the AFM phase. When the Coulomb interaction becomes stronger the mobility increases (cf. Fig. 2) up to the transition point to the AFM phase, which is indicated by the change of slope. In the AFM state one obtains the well-known reduction of the effective bandwidth for large U.

B. The $\delta \neq 0$ case

Upon doping, the situation is much more elaborate. Searching for saddle-point solutions one has to consider other broken-symmetry states like incommensurate CDW, spiral magnetic order, or inhomogeneous phase-separated states besides the simple (π,π) modes. In fact it was demonstrated by Frésard, Dzierzawa, and Wölfle,[15] and more recently by Arrigoni and Strinati[21] that spiral magnetic states lower the AFM free energy at finite doping δ. However the free energy of these much more complicated twisted spin structures exhibits at least qualitatively the same instability against phase separation as the two sublattice AFM solutions. To keep the problem tractable in view of the additional electron-phonon coupling, we restrict ourselves further to the (π,π)-breathing mode (but allow the possibility of phase separation). The standard way to work out the ground-state phase diagram in this restricted sense consists of two steps.[21-23] First, one has to check the relative stability of several homogeneous phases by computing their free energy. Second, we turn to the question of whether the phases identified by us are thermodynamically unstable against phase mixing.

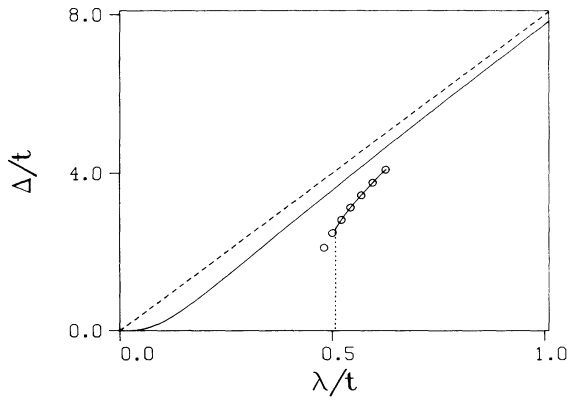

FIG. 3. Lattice displacement Δ vs electron-phonon coupling strength λ at $\delta=0$ for $U=0$ (full line) and $U=4$ ($\triangle$). The jump in Δ at a critical λ (dotted line) indicates a first-order phase transition. The dashed line $\Delta=8\lambda$ gives the asymptotic behavior at $\lambda \gg U,t$.

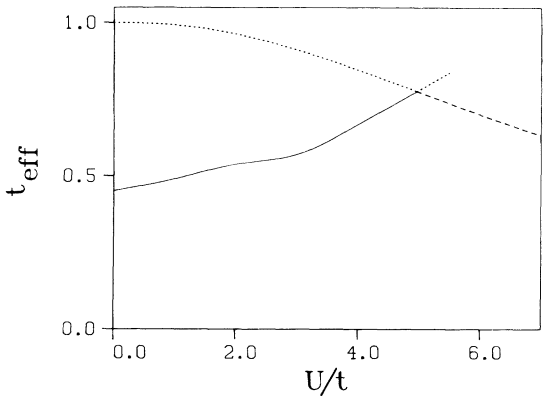

FIG. 4. The effective hopping amplitude t_{eff} vs Coulomb interaction at half filling. Solid line, "dimerized" phase; dashed line, AFM phase; dotted lines, both solutions in their instability region.

Along this line, we first discuss in Figs. 5 and 6 the general qualitative features of homogeneous solutions for lattice displacement and free energy vs U away from half filling at $\lambda=0.625$. In the small δ limit (Fig. 5), one observes the monotonous decrease of Δ as function of U and a metastable "dimerized" solution just above U_c. Δ and U_c are reduced compared to the undoped case. The energy gain relative to the homogeneous AFM and PM solutions and even to spiral magnetic state (here we are able to compare with the free energy given at $U=4$ in Ref. 15) can be seen in both figures. The interesting point is that now the solution with static lattice displacement exhibits ferrimagnetic long-range order in a large region. This becomes evident looking at the mean occupation numbers on both sublattices. When the Coulomb interaction is raised above $U=0.02$ for $\delta=0.05$, the relation $m_A \gg |m_B| \gtrsim 0$ holds until the transition to the "undimerized" solution takes place. This tendency is continued at still larger doping $\delta=0.15$. The "dimerized" solution has the lowest free energy below a critical U_c; however, no free-energy crossover point exists as in the cases

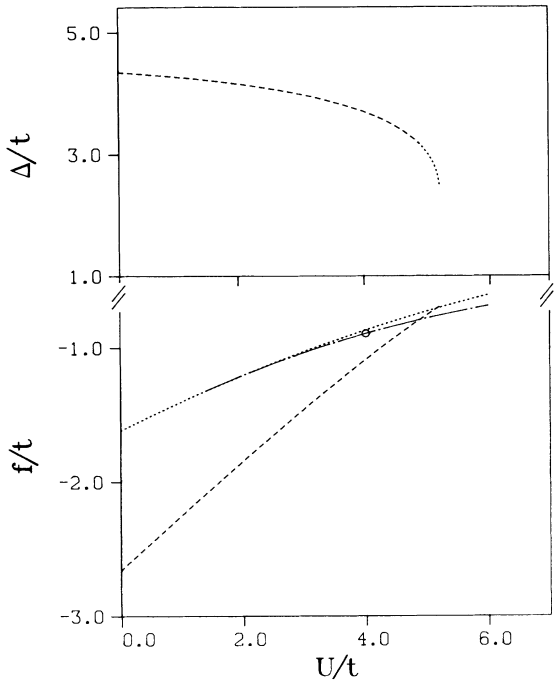

FIG. 5. The U dependence of the static lattice displacement Δ and the free energy f is given away from half filling (dashed curve) at $\delta=0.05$ for $\lambda=0.625$. The free energy of the "dimerized" state is compared with the AFM state (chain dotted line) and the PM state (dotted line) enforced at the same hole concentration. ○ indicates the free energy of the spiral structure with wave vector $Q=(\pi-\delta Q,\pi)$ given in Ref. 15.

of small λ at $\delta=0$. The occupation numbers again show two transition points. The first takes place at $U\approx 0.2$, where the spin structure changes from PM to FIM. The second transition is observed at larger U from the "dimerized" FIM to a solution with zero gap parameter Δ. This transition is of first order. Of course, the exact location of the phase boundary between "dimerized" and "undimerized" phases depends on the variety of states we take into account in minimizing the ground-state energy of the electronic part of the Peierls-Hubbard model.

Doping holes leaves e_B^2 nearly unchanged, whereas the number of double occupied states on the A lattice is reduced, so we have $d_A^2 < e_B^2$ in contrast to $\delta=0$ where $d_A^2=e_B^2$ (see Fig. 7). In consequence, both m_A and m_B ($|m_B|<m_A$) grow smoothly up from zero as the model is doped away from half-filling. In the low doping regime the resulting magnetization becomes proportional to δ. The tendency toward FIM is related to the competition of antiferromagnetic exchange interaction (at large U), the CDW instability due to the local Holstein coupling, and the kinetic energy of the holes (electrons), which favor a FM background. At half-filling, depending on the ratio U/λ, the CDW or AFM state is lowest in energy. Upon doping, the tendencies mentioned above may be at least partially satisfied by magnetic structures representing a compromise,[15] such as the FIM with finite "dimerization."

To analyze the phase diagram in more detail, and address the question of phase mixing, one has to investigate the dependency of the free energy on the electron or hole density. We show in Fig. 8 the free energies obtained

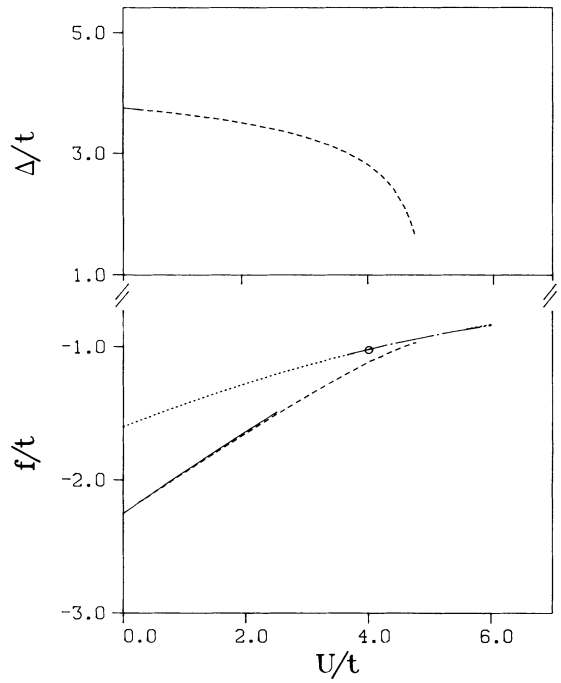

FIG. 6. Static displacement Δ and free energy f of the ground state at doping level $\delta=0.15$ for $\lambda=0.625$. Depending on U, the state with finite Δ exhibits paramagnetic (full line) or ferrimagnetic (dashed line) order. The free energies of the AFM, PM, and spiral states ($\Delta=0$) are given as in Fig. 4.

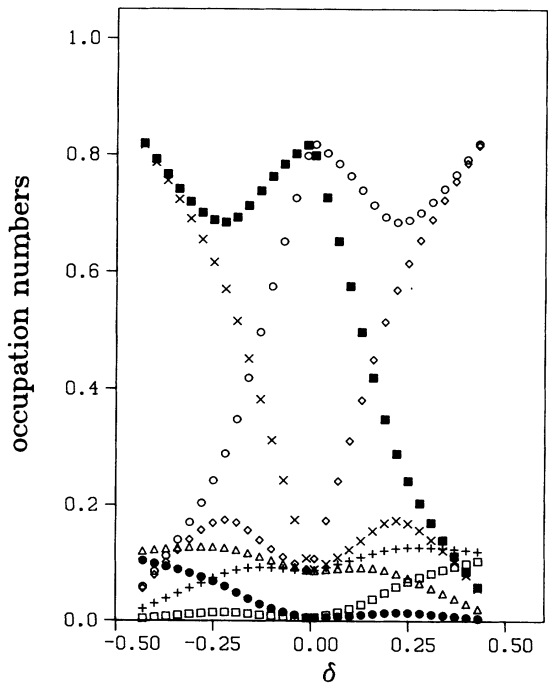

FIG. 7. The occupation numbers e_A^2 (□), d_A^2 (■), $p_{A\uparrow}^2$ (◇), $p_{A\downarrow}^2$ (△), e_B^2 (○), d_B^2 (●), $p_{B\uparrow}^2$ (+), and $p_{B\downarrow}^2$ (×) as a function of doping δ at $U=4$ and $\lambda=0.625$.

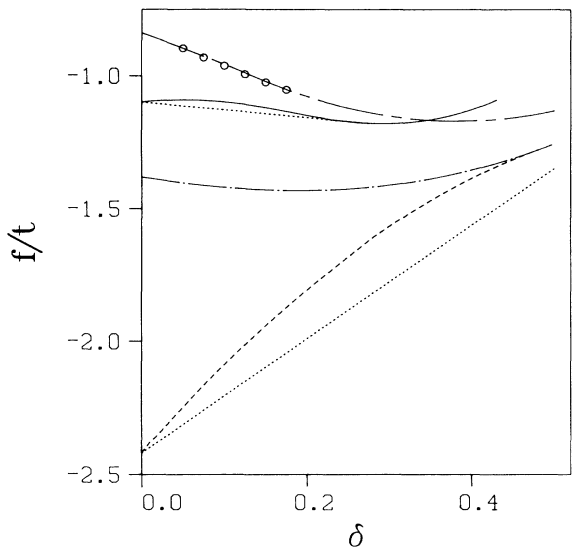

FIG. 8. Free energy as a function of hole concentration δ in a state with (without) static lattice displacement Δ for $U=1$ marked by dashed (chain dotted) curve, and $U=4$ given by a full (chain dashed) curve, where $\lambda=0.625$. The dotted lines denote the two-phase region; ○ denote the free energy for the homogeneous spiral state quoted from Ref. 15.

from "dimerized," spiral, AFM, and PM solutions, for $\lambda=0.625$ and $U=1,4$ as functions of hole density δ. On general stability arguments the free energy of a homogeneous system should be a convex function of the density; otherwise a phase-separated state can be obtained by a Maxwell construction. The existence of a phase-separated state at low hole concentrations was suggested by Visscher[24] for the Hubbard model and recently by Emery, Kivelson, and Lin[25] for the related t-J model;[3] however, until now this point has been rather controversial.[26,27] Mean-field SB approaches to the t-J and Hubbard model yield concave curvature of the free energy in certain parameter regions[15,28,29] [cf. the chain dashed curve (circles) for the AFM (spiral[15]) solution at $U=4$ in Fig. 8]. The boundary of thermodynamic instability is related to the divergence of the isothermal compressibility, i.e., the derivate $\partial\mu/\partial n$ goes to zero. Including the local electron-phonon coupling, the results reported in Fig. 8 show that our uniform "dimerized" saddle-point solution becomes energetically unstable below a critical hole concentration δ_c. Assuming that in this region the system would separate into a hole-rich phase and a phase without holes, the free energy of such a two-phase system can be obtained from

$$f_{II}(\delta)=f(0)+\delta\frac{f(\delta_c)-f(0)}{\delta_c} . \tag{11}$$

Here $f(\delta_c)$ denotes the free energy per site in the hole-rich phase with hole concentration δ_c. The critical concentration δ_c is determined from the minimum of the function $e(\delta)=[f(\delta)-f(0)]/\delta$. That is equivalent to performing a Maxwell construction for the anomalous in-

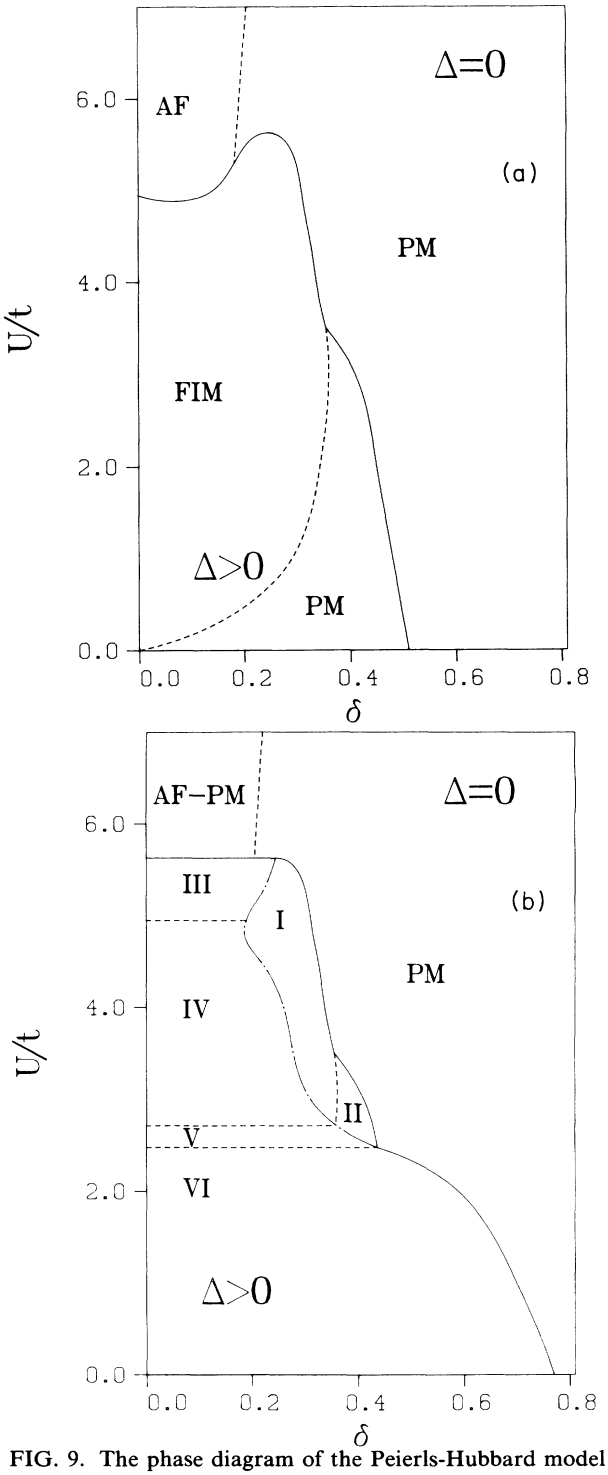

FIG. 9. The phase diagram of the Peierls-Hubbard model is calculated in the δ-U plane at $\lambda=0.625$, where (a) only particular homogeneous states (see text) are taken into account, and (b) phase separation is allowed. The solid line separates "dimerized" from "undimerized" states; dashed lines denote the boundaries between phases with different magnetic order. In Fig. 8(b), the chain dotted line gives the boundary between homogeneous "dimerized" phases with FIM (I) or PM (II) order and the phase-separated regime. The two-phase region is built up by the phases at $\delta=0$ and the states on the right boundary of the respective region; i.e., at $\Delta=0$, AFM-PM, and at $\Delta\neq0$, AFM-FIM (III), PM-FIM (IV), and PM-PM (V, VI).

crease of the chemical potential μ with doping.[21,28,30] The validity of Eq. (11) is restricted to the region $\delta \leq \delta_c$. Let us emphasize that the hole concentration of the hole-rich phase is fixed at δ_c in the phase-separated regime. Reducing δ, the portion of the hole-rich phase becomes smaller. The occupation numbers and Δ for the phase without holes are shown in Figs. 1 and 2.

Finally, the ground-state phase diagram of the Peierls-Hubbard model calculated within our SB scheme is presented in Fig. 9 in the δ-U plane at $\lambda=0.625$. If we admit only homogeneous phases, we get the domains of stability shown in the upper part [Fig. 9(a)]. The solution with finite "dimerization" gives the lowest free energy in a considerable parameter region of U and δ. Increasing the Coulomb interaction, this solution becomes magnetically ordered (FIM) until it breaks down above $U_c(\delta)$. The transition between the two "dimerized" states is of first order, where we were unable to resolve the jump in Δ at lower U values ($U<0.1$). If the magnetic order changes on the boundary, we found that the transition between "dimerized" and "undimerized" solutions is also of first order, otherwise we observe a second-order transition. The inclusion of spiral magnetic phases has only little influence on the extension of the "dimerized" region (cf. Fig. 8). When we allow the possibility of heterogeneous mixing of phases we get the much more complex phase diagram shown in Fig. 9(b). At $n=1$ ($\delta=0$) one has a stable paramagnetic "dimerized" state up to $U_c=4.95$ [cf. Sec. III A and Fig. 9(a)], where the AFM becomes the ground state. Away from half-filling we can distinguish at a first glance four domains: phase-separated regions with (III to VI) and without (AFM-PM) "dimerization," homogeneous states with finite Δ, (I,II), and the pure paramagnetic phase (PM). The two-phase domains are built up by the states at half-filling and the respective phase on the right phase boundary of each region. One can easy check that no mixing of $\delta<0$ and $\delta>0$ phases is possible.[21,22,30] Let us first emphasize that for the case $\Delta=0$ the doped AFM is never stable, and the AFM-PM phase-separated state does extend beyond the AFM/PM boundary of Fig. 9(a). This is in accordance with previous findings for the ground-state phase diagram of the infinite dimensional Hubbard model.[22] The phase-separated domain with $\Delta\neq 0$ is divided again in four regions, where with increasing U the magnetic order of the two coexisting phases changes from PM-PM (VI,V), PM-FIM (IV), to AFM-FIM (III). The gap parameter is finite (but different) for both phases in the regimes IV and V, whereas it vanishes for one constituent in regions III (AFM at $\delta=0$) and VI (PM at $\delta=\delta_c$). It is remarkable that we get stable homogeneous phases with finite Δ in the domains I and II. Especially, we found magnetic order (FIM) in a parameter regime (I) where in the phase diagram of the pure Hubbard model[22,30] no magnetic solutions exists. That means upon doping, the local electron-phonon coupling λ can induce (or stablize) a magnetic ordered state. Further investigations[30] show that a variation of λ shifts only the boundary between the domains with and without "dimerization" [solid curve in Fig. 9(b)], but leaves the qualitative features of the phase diagram unchanged. Even the inclusion of spiral spin states[15,21] should not alter the main predictions of Fig. 9. Of course, at this stage of theory we cannot rule out that other phases such as incommensurate CDW accompanied by more exotic spin structures, e.g., magnetic textures,[31] may yield still lower free energy at a low doping level. However, an adequate treatment of such states leads to tremendous complications in the numerical evaluation of the resulting free-energy functional. Work along this line is in progress.

IV. CONCLUSION

Let us summarize the main results of this paper, obtained from an extended SB mean-field approach to the 2D Peierls-Hubbard model. In the half-filled-band case, the local electron-phonon coupling gives rise to a stable paramagnetic start with a frozen-in on-site lattice displacement. The interplay between electron-phonon and Coulomb correlations leads to a decrease of the gap parameter with increasing Hubbard interaction U. At a critical U_c, a first-order transition to an "undimerized" AFM state takes place, where the electronic correlations reduce U_c below the Hartree-Fock value U_0.

Away from half-filling, one finds "dimerized" states with PM and FIM order to be lowest in energy; i.e., by increasing the hole concentration the Holstein coupling can stablize magnetic solutions. In the low-doping regime the observed concave curvature of the free energy indicates the possibility of a phase-separated state, where below a critical hole density a separation into "dimerized" phases with and without holes takes place. The free energy of such a two-phase system was obtained by a Maxwell construction. The existence of phase separation was also suggested in a wide U parameter regime of the pure Hubbard model[24,25] (i.e., without electron-phonon coupling). However, in actual physical systems the long-range part of the Coulomb interaction, not accounted for in the simple Hubbard model, will try to suppress different carrier densities on a macroscopic scale.[22,27] The question of whether or not phase separation is stable against variations of the Peierls-Hubbard model, for instance against the incorporation of interatomic Coulomb interaction, is planned to be worked out in a subsequent paper.[30]

ACKNOWLEDGMENTS

We are grateful to K. Fesser, V. Waas, D. Ihle, H. Röder, and A. Muramatsu for valuable discussions. Parts of the numerical calculations have been performed at HLRZ, c/o KFA Jülich under Project hbt032.

[1]I. G. Bednorz and K. A. Müller, Z. Phys. B **64**, 189 (1986).
[2]P. W. Anderson, Science **235**, 1196 (1987).
[3]T. M. Rice, J. Less-Common. Met. **164–165**, 1439 (1990).
[4]L. F. Mattheiss, Phys. Rev. Lett. **58**, 1028 (1987); W. Weber, *ibid.* **58**, 1371 (1987).
[5]P. Prelovšek, T. M. Rice, and F. C. Zhang, J. Phys. C **20**, L229 (1987).
[6]A. S. Alexandrov, Phys. Rev. B **38**, 925 (1988); B. K. Chakravarty, D. Feinberg, Z. Hang, and M Avignon, Solid State Commun. **64**, 1147 (1988); R. Micnas, J. Ranninger, and S. Robaszkiewicz, Rev. Mod. Phys. **62**, 113 (1990); J. Ranninger, Z. Phys. B **84**, 167 (1991).
[7]A. N. Das, J. Konior, and D. K. Ray, Physica C **170**, 215 (1990).
[8]A. Bussmann-Holder, H. Büttner, and A. Simon, Phys. Rev. B **39**, 207 (1989); A. Bussmann-Holder, A. Migliori, Z. Fisk, J. L. Sarrao, R. G. Leisure, and S.-W. Cheong, Phys. Rev. Lett. **67**, 512 (1991).
[9]T. Holstein, Ann. Phys. **8**, 343 (1959).
[10]A. Muramatsu and W. Hanke, Physica C **153**, 229 (1988).
[11]F. C. Zhang and P. Prelovšek, Phys. Rev. B **37**, 1569 (1988).
[12]S. Tang and J. E. Hirsch, Phys. Rev. B **37**, 9546 (1988); S. Mazumdar, *ibid.* **39**, 12 324 (1988); S. Tang and J. E. Hirsch, *ibid.* **39**, 12 327 (1989).
[13]A. Prêtre and T. M. Rice, J. Phys. C **19**, 1365 (1986).
[14]G. Kotliar and A. E. Ruckenstein, Phys. Rev. Lett. **57**, 1362 (1986).
[15]R. Frésard, M. Dzierzawa, and P. Wölfle, Europhys. Lett. **15**, 325 (1991); R. Frésard and P. Wölfle (unpublished).
[16]L. Lilly, A. Muramatsu, and W. Hanke, Phys. Rev. Lett. **65**, 1379 (1990); L. Lilly, Ph.D. thesis, University of Würzburg, 1991.
[17]T. Li, P. Wölfle, and P. J. Hirschfeld, Phys. Rev. B **40**, 6817 (1989).
[18]D. Schmeltzer and A. R. Bishop, Europhys. Lett. **12**, 369 (1990).
[19]J. W. Negele and H. Orland, *Quantum Many-Particle Systems* (Addison-Wesley, Reading, MA, 1988).
[20]W. P. Su, J. R. Schrieffer, and A. J. Heeger, Phys. Rev. Lett. **42**, 1698 (1979).
[21]E. Arrigoni and G. C. Strinati, Phys. Rev. B **44**, 7455 (1991).
[22]P. Fazekas, B. Menge, and E. Müller-Hartmann, Z. Phys B **78**, 69 (1990).
[23]L. D. Landau and E. M. Lifschitz, *Course of Theoretical Physics* (Pergamon, Oxford, 1980), Vol. 5.
[24]P. B. Visscher, Phys. Rev. B **10**, 943 (1974).
[25]V. J. Emery, S. A. Kivelson, and H. Q. Lin, Phys. Rev. Lett. **64**, 475 (1990).
[26]A. Moreo, D. Scalapino, and E. Dagotto, Phys. Rev. B **43**, 11 442 (1991).
[27]H. Fehske, V. Waas, H. Röder, and H. Büttner, Solid State Commun. **76**, 1333 (1990); H. Fehske, V. Waas, H. Röder, and H. Büttner, Phys. Rev. B **44**, 8473 (1991).
[28]M. Uchinami, Phys. Rev. B **42**, 10 178 (1990).
[29]T. I. Ivanov, Phys. Rev. B **44**, 12 077 (1991).
[30]M. Deeg, H. Fehske, and H. Büttner (unpublished).
[31]A. R. Bishop, F. Guinea, P. S. Lomdahl, E. Louis, and J. A. Vergés, Europhys. Lett. **14**, 157 (1991).